INL/CON-06-11914
PREPRINT

U-Mo Foil/Cladding Interactions in Friction Stir Welded Monolithic RERTR Fuel Plates

26th International Meeting on Reduced Enrichment for Research and Test Reactors

D.D. Keiser, Jr.
J.F. Jue
C.R. Clark

October 2006

U-Mo Foil/Cladding Interactions in Friction Stir Welded Monolithic RERTR Fuel Plates

[1]

by

D. D. Keiser, Jr., J. F. Jue, and C. R. Clark

Idaho National Laboratory

P. O. Box 1625

Idaho Falls, ID 83403-6188

Paper to be presented at the 26th International Meeting on Reduced Enrichment for

Research and Test Reactors

Cape Town, South Africa

October 29-November 2, 2006

[1] Work supported by the U.S. Department of Energy, Office of Nuclear Materials Threat Reduction (NA-212), National Nuclear Security Administration, under DOE-NE Idaho Operations Office Contract DE-AC07-05ID14517.

U-MO FOIL/CLADDING INTERACTIONS IN FRICTION STIR WELDED MONOLITHIC RERTR FUEL PLATES

D.D. KEISER, JR., J. F. JUE, and C. R. CLARK
Idaho National Laboratory, P.O. Box 1625, Idaho Falls, ID 83403-6188, USA

ABSTRACT

Interaction between U-Mo fuel and Al has proven to dramatically impact the overall irradiation performance of RERTR dispersion fuels. It is of interest to better understand how similar interactions may affect the performance of monolithic fuel plates, where a uranium alloy fuel is sandwiched between aluminum alloy cladding. The monolithic fuel plate removes the fuel matrix entirely, which reduces the total surface area of the fuel that is available to react with the aluminum and moves the interface between the fuel and cladding to a colder region of the fuel plate. One of the major fabrication techniques for producing monolithic fuel plates is friction stir welding. This paper will discuss the interactions that can occur between the U-Mo foil and 6061 Al cladding when applying this fabrication technique. It has been determined that the time at high temperatures should be limited as much as is possible during fabrication or any post-fabrication treatment to reduce as much as possible the interactions between the foil and cladding. Without careful control of the fabrication process, significant interaction between the U-Mo foil and Al alloy cladding can result. The reaction layers produced from such interactions can exhibit notably different morphologies vis-à-vis those typically observed for dispersion fuels.

1. Introduction

Interactions between U-Mo particles and Al matrix in RERTR dispersion fuels can drastically impact the overall in-reactor performance of these fuels [1]. As a result, it is of particular interest to determine how U-Mo/Al alloy cladding interactions may impact the performance of U-Mo monolithic fuels. Interaction between the fuel foil and cladding in monolithic fuels can transpire either during fabrication or during irradiation. When considering fabrication, a major technique being evaluated for producing RERTR monolithic fuel plates is friction stir welding (FSW) [2]. Any interaction layers that are generated during FSW, will be present in fuel plates when they are inserted into a reactor.

For the FSW process, a rotating tool is impinged onto the surface of a fuel plate and drawn across the plate. The heat and friction caused by this contact produces localized plastic deformation of the surface of the 6061 Al used as cladding material, allowing the tool to be forced into the cladding. Travel of the imbedded tool results in displacement of material and creation of a weld. Construction of a fuel plate requires several overlaying lap welds to bond the cladding plate faces together and to bond the cladding to the fuel foil. The welding action, as the rotating tool passes over the foil, smears the aluminum cladding onto the foil giving good interfacial contact. Since temperature will affect the interactions between the fuel and cladding, the temperature should be kept as low as possible. When butt-welding 6061 Al, the maximum temperature a work piece is exposed to at the weld center is around 450˚C for a few minutes [3]. By incorporating water cooling into the FSW equipment this temperature can be reduced and kept more consistent.

To investigate fuel/cladding interactions in monolithic plates fabricated by FSW, various samples were taken from as-fabricated plates that were later heated to produce fuel/cladding interaction zones that were large enough to characterize. Characterization was performed using optical metallography (OM) and scanning electron microscopy (SEM) combined with energy dispersive spectroscopy (EDS) and wavelength dispersive spectroscopy (WDS). This paper will describe the results from these characterizations and how the fuel/cladding interaction behavior changes depending on whether the foil in the FSW monolithic plate is U-7Mo or U-10Mo.

2. Results

For the FSW samples, an annealing step was applied at 500˚C or 550˚C to promote interactions between the fuel and cladding. Table 1 lists those samples that were annealed, sliced into transverse cross sections, and then characterized. The FSW samples that were tested consisted of a 250-μm U-Mo foil and 6061 Al or 1100 Al cladding. 6061 Al is nominally comprised of 0.4 to 0.8 wt% Si, 0.7 wt% Fe, 0.15 to 0.4 wt% Cu, 0.15 wt% Mn, 0.8 to 1.2 wt% Mg, 0.04 to 0.35 wt% Cr, 0.25 wt% Zn, 0.15 wt% Ti, and bal. Al. 1100 Al is nominally comprised of 1.0 wt% (Fe+Si), 0.05 to 0.20 wt% Cu, 0.05 wt% Mn, 0.10 wt% Zn, and bal. Al.

Table 1. Characterized Fuel Samples.

Label	Fuel Composition (Wt%)	Al Alloy Cladding	Annealing Temp. (˚C)	Annealing Time (Hr)
N1F070	U-7Mo	6061	500	0.5
N1F070b	U-7Mo	6061	500	0.5
N1F080	U-7Mo	6061	500	0.5
L1F110	U-10Mo	6061	500	0.5
L1F080	U-10Mo	6061	500	0.5
A*	U-10Mo	6061	550	100
B	U-10Mo	1100	550	2
C	U-10Mo	1100	550	5

* Labels A, B, and C were created for sample tracking.

2.1 U-7Mo Plates

Figure 1 shows the typical microstructures observed for fuel plates N1F070 and N1F080. Significant fuel/cladding interaction (FCI) has occurred between the U-7Mo fuel and the Al-6061 cladding during the 500˚C, 30 min. annealing treatment. Some areas of the fuel plates had more significant interaction than others, as shown in Figure 2. The result is the presence of a relatively large, uniform uranium-aluminide layer. Figure 3 shows how uranium-aluminide forms as a result of uranium-aluminum interdiffusion along grain and phase boundaries. The γ-phase seems to have decomposed to α-U and U_2Mo phase in localized areas during the fabrication and annealing treatment. At the center of the U-Mo foil, Al was found in a precipitate phase (see Fig. 4). Point-to-point composition analysis showed that the Al-rich phase at the fuel center had an approximate composition, in at%, of 60U-10Mo-26Al-4Si. Two different types of interaction layers were observed at the fuel/cladding interface based on morphology and Si behavior. The first layer, shown in Figure 5, was present near areas in the fuel where the γ-phase had decomposed. Based on composition, $(U,Mo)(Al, Si)_3$, and $(U,Mo)(Al,Si)_4$ phases seem to comprise this diffusion zone, and both phases contain negligible Si. The second type of interaction zone is much narrower and contains appreciable Si (see Fig. 6). No evidence of γ-phase decomposition was observed near this type of interaction layer. Point to point analysis of the layer nearest the fuel/cladding interface revealed the following ranges in U, Mo, Al, Si content (at%): (23-35)U, (4-5)Mo, (11-60)Al, (12-47)Si.

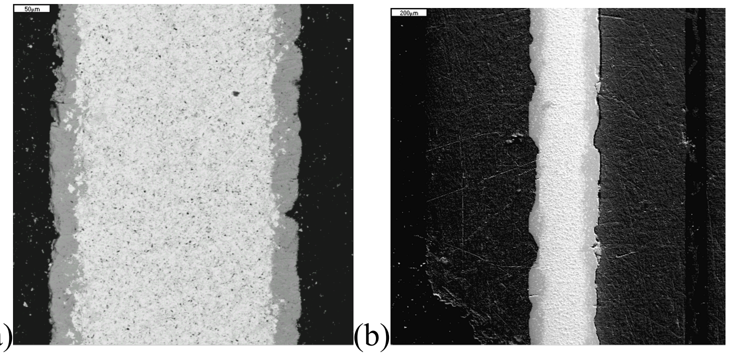
(a) (b)

Figure 1. SEM backscattered electron micrograph of the typical microstructure observed for fuel plate (a) N1F070 and (b) N1F080. A relatively large uranium-aluminide layer (medium contrast) region is observed. The black region is the 6061 Al alloy and the bright-contrast area is U-7Mo alloy.

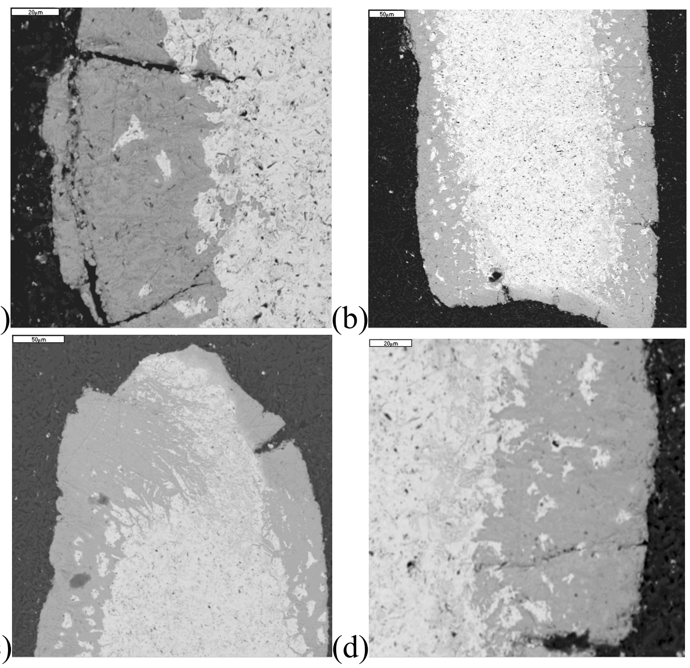
(a) (b) (c) (d)

Figure 2. SEM backscattered electron micrographs (a-d) showing areas in the fuel plate N1F070 where a relatively large uranium-aluminide layer (medium contrast) has formed. The black region is the Al-6061 alloy and the bright-contrast area is U-7Mo alloy. Fuel plate N1F080 exhibited similar areas.

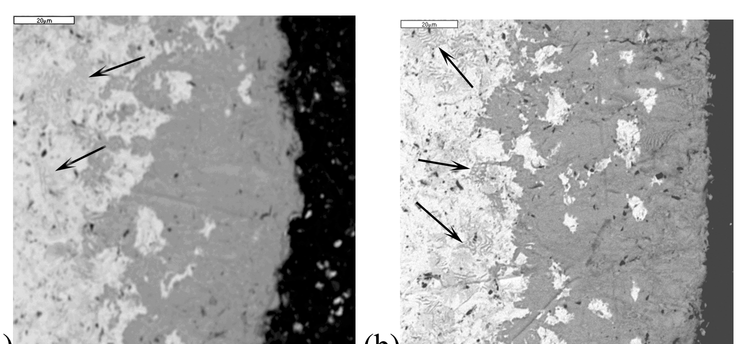
(a) (b)

Figure 3. SEM backscattered electron micrographs (a-b) of the microstructure observed for fuel plate N1F070. Arrows point to regions where γ-phase has transformed to α-U and U_2Mo, and the α-U has reacted with Al.

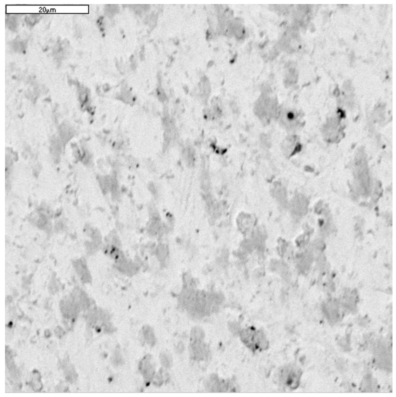

Figure 4. SEM backscattered electron micrograph of the two-phase microstructure observed at the center of the fuel plate. The bright phase is a U-Mo phase. The dark phase is enriched in Al.

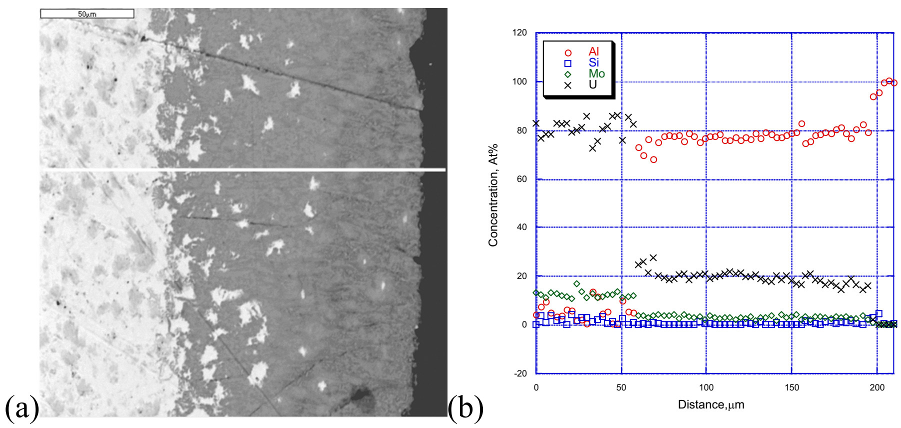

Figure 5. (a) Backscattered electron image and (b) Al, Si, Mo, and U concentration profiles generated along the line shown in (a).

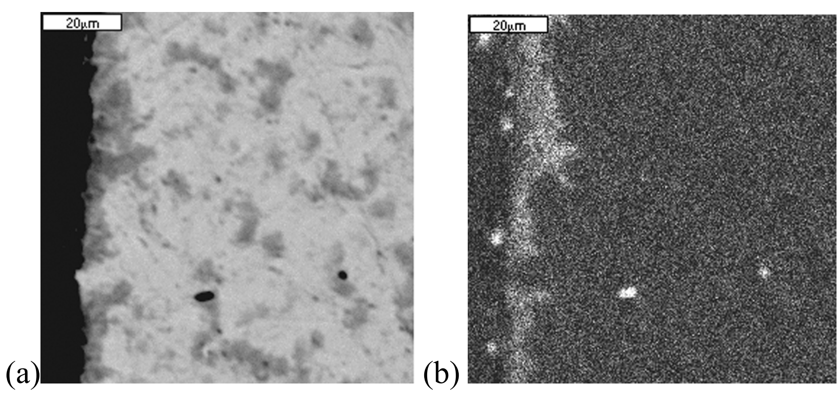

Figure 6. SEM backscattered electron micrograph (a) and (b) X-ray map for Si, where the uranium-aluminide layer contains the highest levels of Si.

2.2 U-10Mo Plates

The fuel interaction zone for sample L1F080, which was annealed at 500˚C for 30 min., is presented in Figure 7. Sample L1F110 exhibited a very similar structure. Higher magnification images indicated that the medium-contrast interaction zone at the fuel/cladding interface consists of two different layers (see Fig. 8). The layer nearest the unreacted cladding contains more Mg and Al than does the other layer (see Fig. 9). Fe, which is a minor component of 6061 Al, was observed in precipitate phases near the fuel/cladding interface and in the interaction layers, in minor concentrations. The Fe is generally contained in different precipitates compared to Si. Point-to-point composition analysis indicated that the interaction layer nearest the unreacted cladding had the following composition ranges for U, Mo, Al, and Si: (14-19)U, (1-4)Mo, (61-71)Al, (10-18)Si, indicating a $(U,Mo)(Al,Si)_3$ or $(U,Mo)(Al,Si)_4$ phase. The other layer had the following composition ranges: (26-31)U, (7-10)Mo, (15-21)Al, (40-45)Si, not clearly indicating any specific type of UAl_x phase. Similar to the FSW samples with U-7Mo alloy, Al was observed to be present in the center of the foil in a precipitate phase (see Fig. 10).

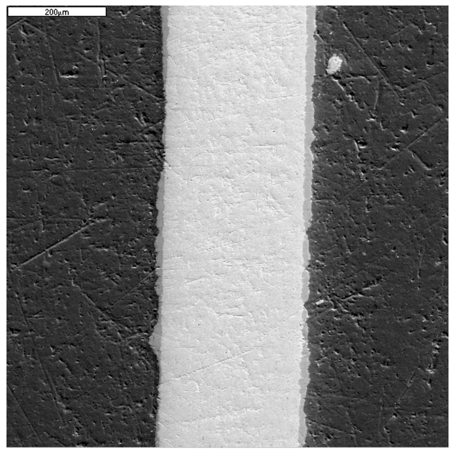

Figure 7. SEM secondary electron micrograph of fuel plate L1F080.

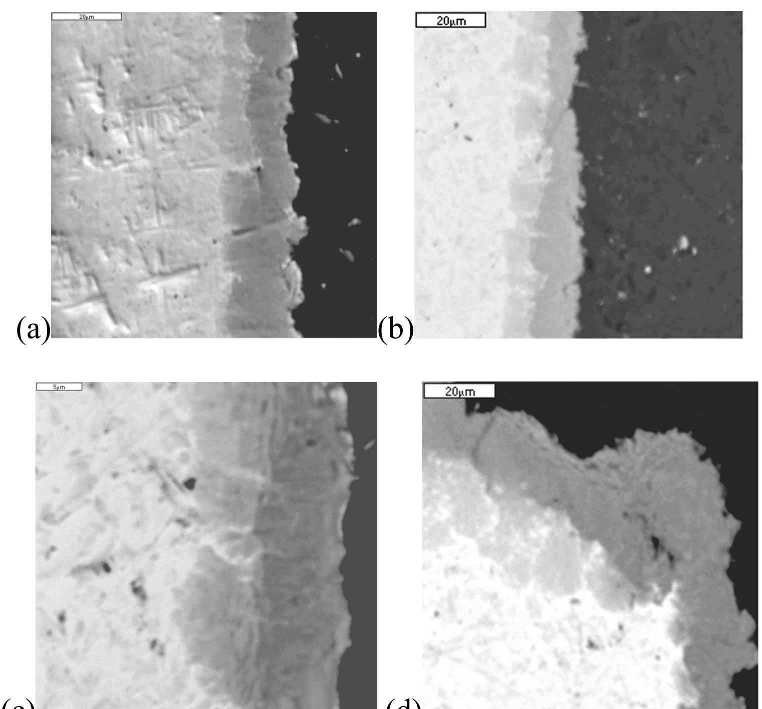

Figure 8. (a) SEM secondary electron image and (b-d) backscattered electron images of the diffusion layers that formed at the fuel/cladding interface in fuel plate L1F080. The bright contrast area in the images is U-10Mo fuel; the medium contrast areas are the interdiffusion layers; and, the black area is 6061 Al.

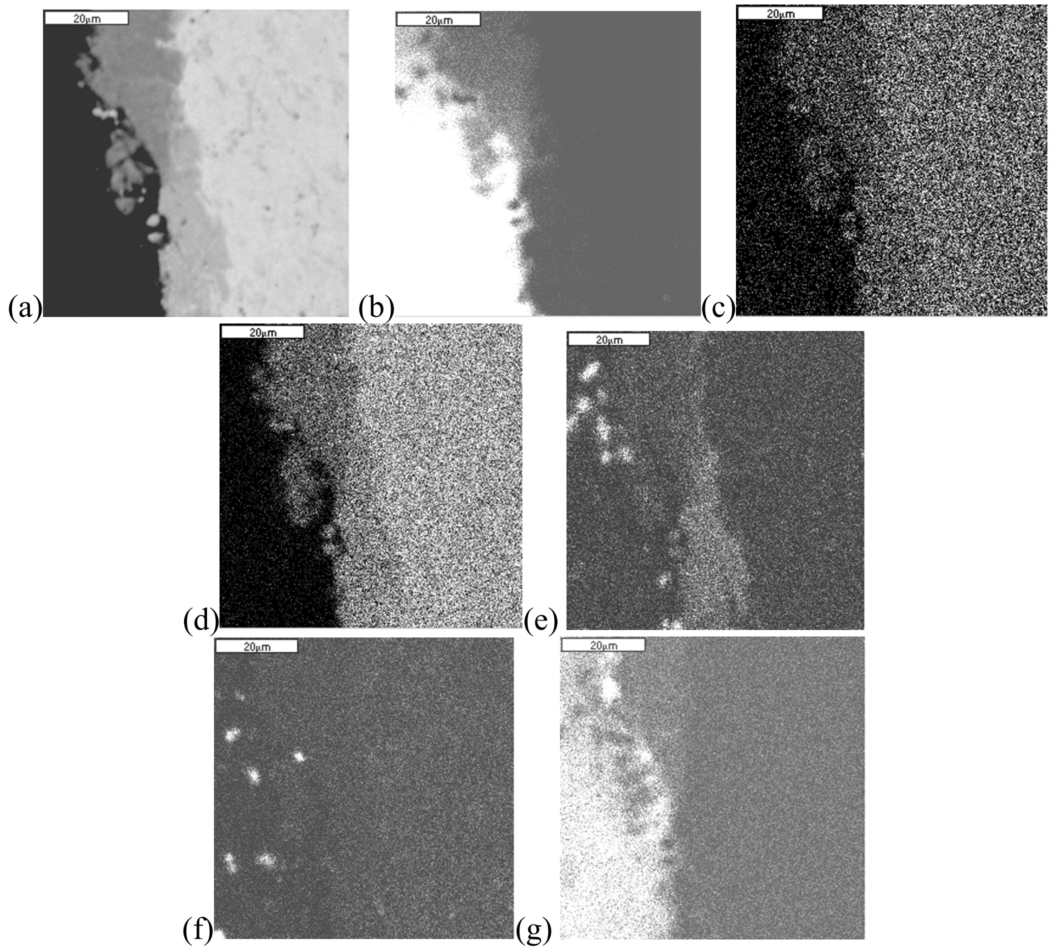

Figure 9. SEM backscattered electron micrograph (a) and X-ray maps for (b) Al, (c) Mo, (d) U, (e) Si, (f) Fe, and (g) Mg.

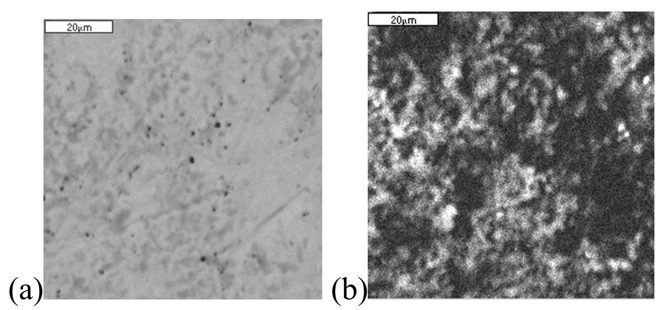

Figure 10. SEM backscattered electron micrograph (a) and (b) Al X-ray map at the center of the L1F080 foil.

Sample A was annealed at 550˚C for 100 hours to investigate the final microstructure that would form over a long timeframe when the diffusion structure that initially developed was like the ones described for samples L1F080 and L1F110. Figure 11 shows the microstructure at the center of the plate where some U-10Mo foil still remains, and the microstructure in areas where the U-10Mo foil has been completely consumed. The fuel/cladding interaction zone is multiphase and has an average composition of between 78 and 80 at.% Al, like that of a $(U,Mo)Al_4$ type of phase. Two fine phases contribute to this average composition: a UAl_3 (75 at% Al) phase and a $(U,Mo)Al_x$ (80 at.% Al) phase. Nearest the unreacted cladding an approximately 10-µm-thick, Al-rich (86 at% Al) layer was identified. In Figure 11d, it can be seen that the original 250-µm-thick foil has been consumed and replaced by an interdiffusion zone with an overall thickness of ~1,000 μm due to the formation of lower density phases.

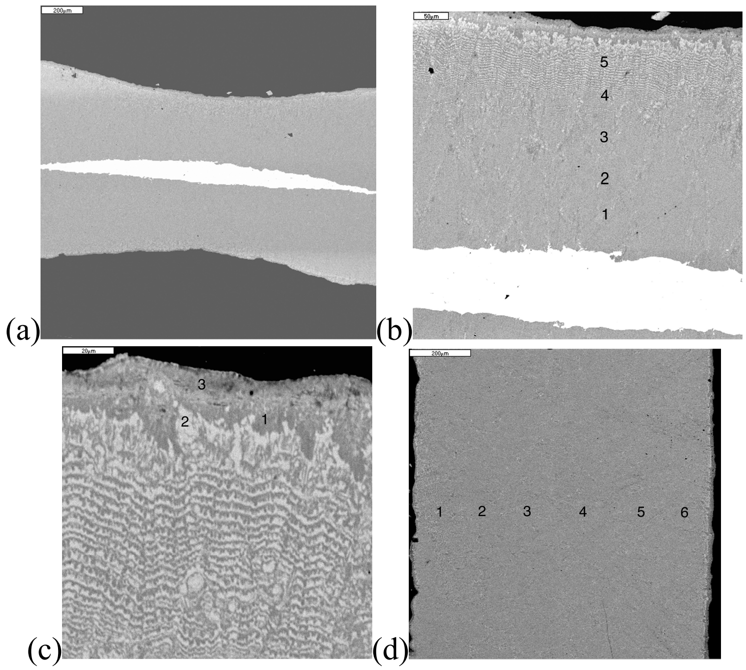

Figure 11. SEM backscattered electron micrographs of Sample A showing (a) a low magnification image of the reaction zone, (b) a higher magnification image of the layers from the remaining U-Mo foil to the unreacted 6061 Al, (c) the area of the interaction zone nearest the unreacted 6061 Al alloy, and (d) an area where the foil was consumed. The numbers identify locations in (b and d) where box-scan analysis was performed and in (c) where point-to-point analysis was performed.

Two samples (B and C) were tested at 550˚C to evaluate the performance of samples with 1100 Al cladding. The observed interaction zones were not of consistent thickness along the fuel/cladding interface, like was the case for the samples with 6061 Al. Figure 12 shows the thickest interaction zones that developed between U-10Mo and 1100 Al in samples annealed for 2 and 5 hours. These interaction zones are similar to the ones observed for samples consisting of U-Mo foils and 6061 Al. The zones had an average Al composition of around 80 at% Al throughout, except nearest the unreacted cladding where an Al-rich phase (85 at% Al) was observed.

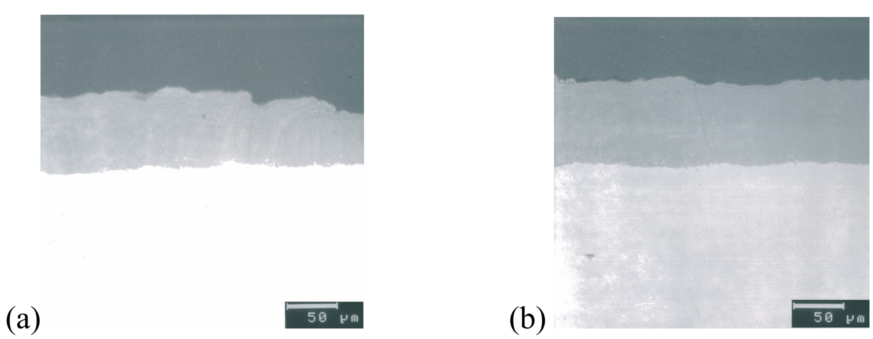

Figure 12. SEM micrograph of FSW sample annealed at 550˚C for (a) 2 hours and (b) 5 hours. The bright contrast region is the U-10Mo fuel. The darkest area is the 1100 Al alloy. The medium contrast area is the $(U,Mo)_{0.9}Al_4$ phase. At the interaction zone/1100 Al interface was observed a 1-2 μm-thick, Al-rich layer.

To gain insight as to the grain structure of the U-Mo foil before FSW, after FSW, and after heat-treating, optical metallography was performed on various samples. Figure 13 shows a U-Mo foil after hot rolling and after cold rolling followed by stress relieving. A heavily textured microstructure is observed in the foils. Figure 14 shows the microstructure of a U-10Mo foil in a FSW plate that was later heat-treated at 385˚C or 500˚C. In the 385˚C sample, the original fine microstructure, which is still present at the center of the foil, exhibits grain growth towards the foil/cladding interface. After heat treatment at 500˚C for 30 minutes an equiaxed structure is produced.

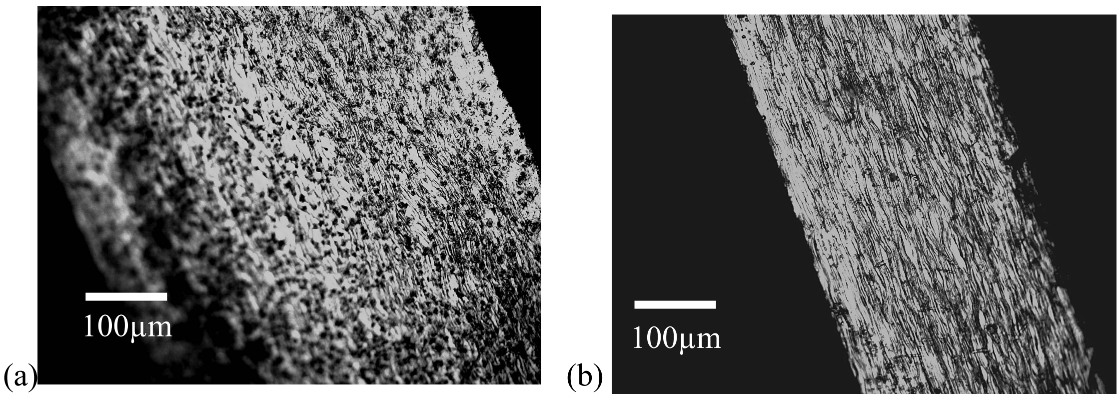

Figure 13. Optical images of (a) a U-10Mo foil after hot rolling and (b) after cold rolling and stress relieving (annealed at ~900˚C for less than a minute).

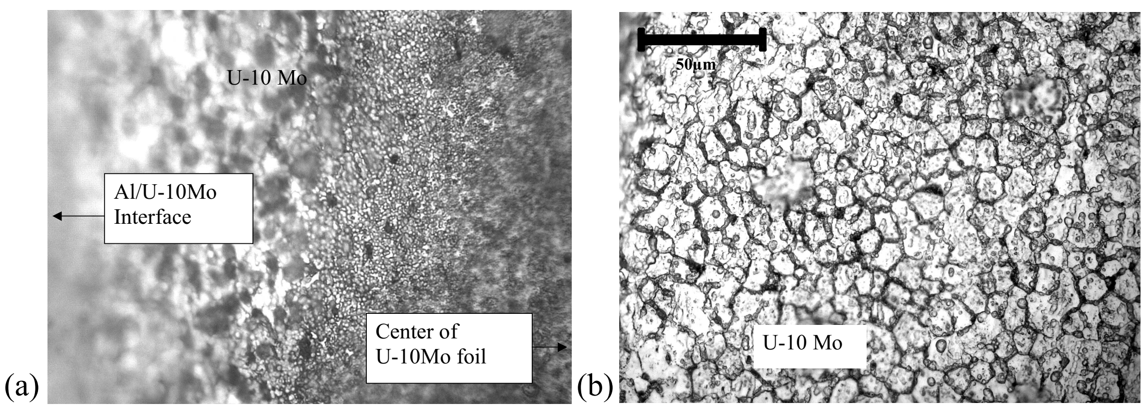

Figure 14. Optical images of (a) a U-10Mo foil contained in a FSW plate that was held at 385˚C for 3 minutes, and (b) one held at 500˚C for 30 minutes.

3. Discussion

The friction stir welding process typically results in the development of three distinct weld zones: a stirred (nugget) zone, a thermo-mechanically affected zone (TMAZ), and a heat-affected zone (HAZ) [3]. Yet, when FSW is applied to fabricate monolithic fuel plates, all of the unwelded regions outside the final fuel plate outline are removed. The resulting microstructure of the 6061 Al is comprised of a homogeneous area that is identified as a TMAZ region. The fine grain structure shows no signs of recrystallization characteristic of the weld nugget and shows grain refinement beyond what is typical for the HAZ. The U-Mo foil retains an as-rolled appearance despite the FSW process [4].

When monolithic fuel plates, with the microstructures described above, are annealed at 500˚C or above, the fuel and cladding interact to produce non-uniform interdiffusion zones. U-7Mo plates develop interaction zones that differ from the ones produced for U-10Mo plates. In some areas, the U-7Mo samples form relatively wide interaction zones comprised of uranium-aluminides that contain negligible Si. In other regions, narrow interaction zones develop that contain appreciable Si. There appears to be a correlation between the decomposition of the γ-phase in a U-7Mo alloy and the type of interaction zones that develop. Conversely, U-10Mo samples develop interaction zones that are comprised of two distinct Si-containing layers, with the most Si-enriched layer forming towards the fuel. Both U-7Mo and U-10Mo foils contain Al in the center of the foil, as an Al-rich precipitate, after annealing at 500˚C.

Results have been reported for diffusion experiments using U-7Mo/6061 Al diffusion couples [5, 6, 7]. In [5], results were reported for a U-7Mo/6061 Al couple annealed at 580˚C for 2 hours. The developed interaction zone was comprised of $U_{20}Mo_2Si_{2\text{-}3}Al_{75\text{-}76}$, and no Si-rich phases were reported to form anywhere along the fuel/Al alloy interface. In another study, negligible interaction was observed in a U-7Mo/6061 Al couple that was annealed at 550˚C for 50 hours [6]. For annealing studies using U-7Mo dispersion fuels with Al-2Si matrix that were annealed at 550˚C for 25 hours, interaction layers with high Si levels were observed. Yet, in samples annealed at 580˚C for 10 hours no Si enrichment was observed in the interaction layer [7]. Comparing the results of these studies with those reported in this paper, it seems that decomposition of the γ-U phase in U-Mo alloys may dictate whether or not a Si-rich phase will form in a U-7Mo/6061 Al couple. Also when the Mo content in a U-Mo alloy is increased from 7 to 10 wt%, then significantly enriched Si layers can develop. In the results from Bozzolo-Ferrante-Smith (BFS) studies of U-Mo alloys interacting with Al-Si alloys [8], it was found that high Si concentrations will reduce Al diffusion into a U-Mo alloy and an unexpected interaction between Mo and Si can inhibit Si diffusion deeper into the U-Mo solid solution, thereby improving the stopping power for Al diffusion. This may help explain the behaviors observed in the annealed U-10Mo FSW samples analyzed in this study.

For the case of the FSW U-10Mo sample annealed at 550˚C for 100 hours, the formed interaction was very similar to those observed for annealed U-7Mo/Al diffusion couples [9,10]. The same periodic layers that form in this sample have been reported in the other diffusion studies, and the Al-rich phase in these studies was found to be UMo_2Al_{20}. Not only the U-10Mo/6061 Al sample annealed for 100 hours but also the U-10Mo/1100 Al samples annealed for 2 to 5 hours developed FCI layers very similar to what forms in the reported U-Mo/Al diffusion couples. This seems to indicate that any unique behaviors that result from the FSW-generated microstructure or that result from the presence of Si, Mg, or Fe in the 6061 or 1100 Al lose their effect over longer time periods at relatively high temperatures. After longer timeframes, the final diffusion structures are very similar to those observed in typical U-Mo/Al diffusion couples. If the annealing temperatures were much lower, the Si in the interaction layers may stay enriched for longer annealing times. In addition, if the Si was at a higher concentration (at least greater than around 1 wt%) in the Al alloy, the Si-enriched layers may remain stable for longer annealing times at a temperature of 500˚C or above. It has been reported that at least 5 wt% Si needs to be present in the Al matrix of dispersion fuels to stabilize a $U(Al,Si)_3$ phase in irradiated fuels over the Al-rich phases that want to develop [11]. Of course, this would be at a much lower temperature than the 500˚C employed for this work. For monolithic fuels fabricated using FSW, a similar Si requirement may be required.

4. Conclusions

Based on the annealing and characterization of monolithic FSW plates the following conclusions can be drawn: (1) during relatively short term anneals at 500˚C, monolithic FSW fuel plates develop FCI structures that exhibit notable differences compared to those that typically form in U-Mo/Al dispersion fuels and U-Mo/Al diffusion couples, and the features of the FCI structures are related to whether the fuel foil is U-7Mo or U-10Mo; (2) longer anneals (2 hours or greater) produce FCI zones that look very similar to those that form in U-Mo/Al dispersion fuels and U-Mo/Al diffusion couples; (3) minor constituents in 6061 Al alloy (e.g., Si, Mg, and Fe) can become enriched in FCI layers; and (4) the presence of Si-rich layers in the interaction zone can reduce the width of uranium-aluminide layers at the fuel/cladding interface and can eliminate the formation of an Al-rich (U, Mo, Al) phase.

Acknowledgments

This work was supported by the U.S. Department of Energy, Office of Nuclear Materials Threat Reduction (NA-212), National Nuclear Security Administration, under DOE-NE Idaho Operations Office Contract DE-AC07-05ID14517.

References

[1] G. L. Hofman et al., 8th International Topical Meeting on Research Reactor Fuel Mangement (RRFM), München, Germany, March 21-24, 2004.
[2] C. R. Clark et al., 8th International Topical Meeting on Research Reactor Fuel Mangement (RRFM), München, Germany, March 21-24, 2004.
[3] R. S. Mishra, Z. Y. Ma, *Mater. Sci. and Engr. R*, **50** (2005) 1.
[4] C. R. Clark et al., 10th International Topical Meeting on Research Reactor Fuel Mangement (RRFM), Sofia, Bulgaria, April 30 –May 3, 2006.
[5] M. Mirandou, M. Granovsky, M. Ortiz, S. Balart, S. Arico, and L. Gribaudo, International Meeting of Reduced Enrichment for Research and Test Reactors (RERTR), Vienna, Austria, November 7-12, 2004.
[6] S. Dubois et al., 9th International Topical Meeting on Research Reactor Fuel Mangement (RRFM), Budapest, Hungary, April 10-13, 2005.
[7] J. M. Park, et al., International Meeting of Reduced Enrichment for Research and Test Reactors (RERTR), Bosston, Massachusetts, USA, November 6-10, 2005.
[8] J. E. Garces, et al., International Meeting of Reduced Enrichment for Research and Test Reactors (RERTR), Bosston, Massachusetts, USA, November 6-10, 2005.
[9] F. Mazaudier, et al., 10th International Topical Meeting on Research Reactor Fuel Mangement (RRFM), Sofia, Bulgaria, April 30 –May 3, 2006.
[10] D. D. Keiser, Jr., *Argonne National Laboratory Report*, ANL 05/14 (2005).
[11] G.L. Hofman, Y.S. Kim, H. J. Ryu, and J. Rest, 10th International Topical Meeting on Research Reactor Fuel Mangement (RRFM), Sofia, Bulgaria, June, 2006.